Annals of Biomedical Engineering, Vol. 24, pp. 606–616, 1996
Printed in the USA.

0090-6964/96 $10.50 + .00

Magnetic Stimulation of the Nervous System: Induced Electric Field in Unbounded, Semi-infinite, Spherical, and Cylindrical Media

PAOLO RAVAZZANI,* JARMO RUOHONEN,† FERDINANDO GRANDORI,* and GABRIELLA TOGNOLA*

*System Theory Center (CNR), Department of Biomedical Engineering, Polytechnic of Milan, Milan, Italy, and
†BioMag Laboratory, Medical Engineering Centre, Helsinki University Central Hospital, Helsinki, Finland

Abstract—Knowledge of the electric field that is induced in the brain or the limbs is of importance in magnetic stimulation of the nervous system. Here, an analytical model based on the reciprocity theorem is used to compare the induced electric field in unbounded, semi-infinite, spherical, and cylinder-like volume conductors. Typical stimulation coil arrangements are considered, including the double coil and various orientations of the single coil. The results can be used to determine when the influence of the boundaries is negligible enough to allow the use of more simplified geometries.

Keywords—Reciprocity theorem, Cortical and peripheral magnetic stimulation, Boundary effects, Medium geometry, Electric field

INTRODUCTION

Following the initial demonstration of human cortical stimulation in 1985 (1), the technique of clinical magnetic stimulation has become widely used for the investigation of the central and the peripheral nervous system in humans. Neural stimulation is achieved only if the target (brain tissues, limbs, thorax) is exposed to a suitable electric field, and hence the amount and distribution of the electric field **E** are of great consequence. The question has already been treated by means of either geometrically approximated models (2,5,7,10,12,23) or accurate mathematical methods (4,6,8,15,16,24,25) to predict the induced electric field and the subsequent current flow. Irrespective of the differences between the mathematical and physical approaches, the two groups of models differ mainly in the geometrical approximation, that is whether or not they take into account the influence of the medium boundaries. Despite the crucial importance of this point in the interpretation of the modeling outcomes, there are no studies that focus on quantification of the relative degree of approximation attributed to geometrical factors. In this study this problem has been approached by means of a flexible model based on the reciprocity theorem, proposed in most recent years by several authors (11,13,18,19,26) to compute the induced electric field in realistically shaped media. After a short introduction of the model and a discussion of some approximation in the results due to the finite dimension of the coil surface, this paper addresses the effects of the medium geometry on the induced electric fields, considering both cortical and peripheral nerve stimulation. The results can be useful in determining the cases in which the influence of the boundaries is negligible enough to allow the use of the most simplified geometries.

Address correspondence to Dr. Paolo Ravazzani, Centro Teoria dei Sistemi (CNR), Department of Biomedical Engineering, Polytechnic of Milan, Via Ponzio 34/5, 20133 Milan, Italy.
(Received 28Dec95, Accepted 15Feb96)

THE MODEL

Theoretical Considerations

An analytical model based on the reciprocity theorem was first mentioned by Yonokuchi *et al.* (26) and by Cohen and Cuffin (2). They limited their discussion to unbounded and semi-infinite media. Later, Heller and van Hulsteyn (11) gave the explicit equations for spherical media, in the study of cortical stimulation, and more recently Grandori and coworkers (13,18,19) have extended the model to a cylindrical medium, mimicking peripheral nerve stimulation. On practical grounds, the induced electric field **E** in a point P inside any reciprocal medium is estimated by means of the magnetic induction **B** produced outside the medium by a current dipole **Q** located at the point P. Thus, the estimation of **E** is reduced to the computation of the magnetic induction **B**, *i.e.*, to the solution of the so-called biomagnetic forward problem. This problem is well discussed in literature, at least for the geometries usually considered in modeling of magnetic stimulation, that is, unbounded and semi-infinite medium, sphere and cylinder (3,22).

Here, in short, one can find the main steps of the mathematical approach. Let us consider a current loop C in which a sinusoidal current i of angular frequency ω flows,

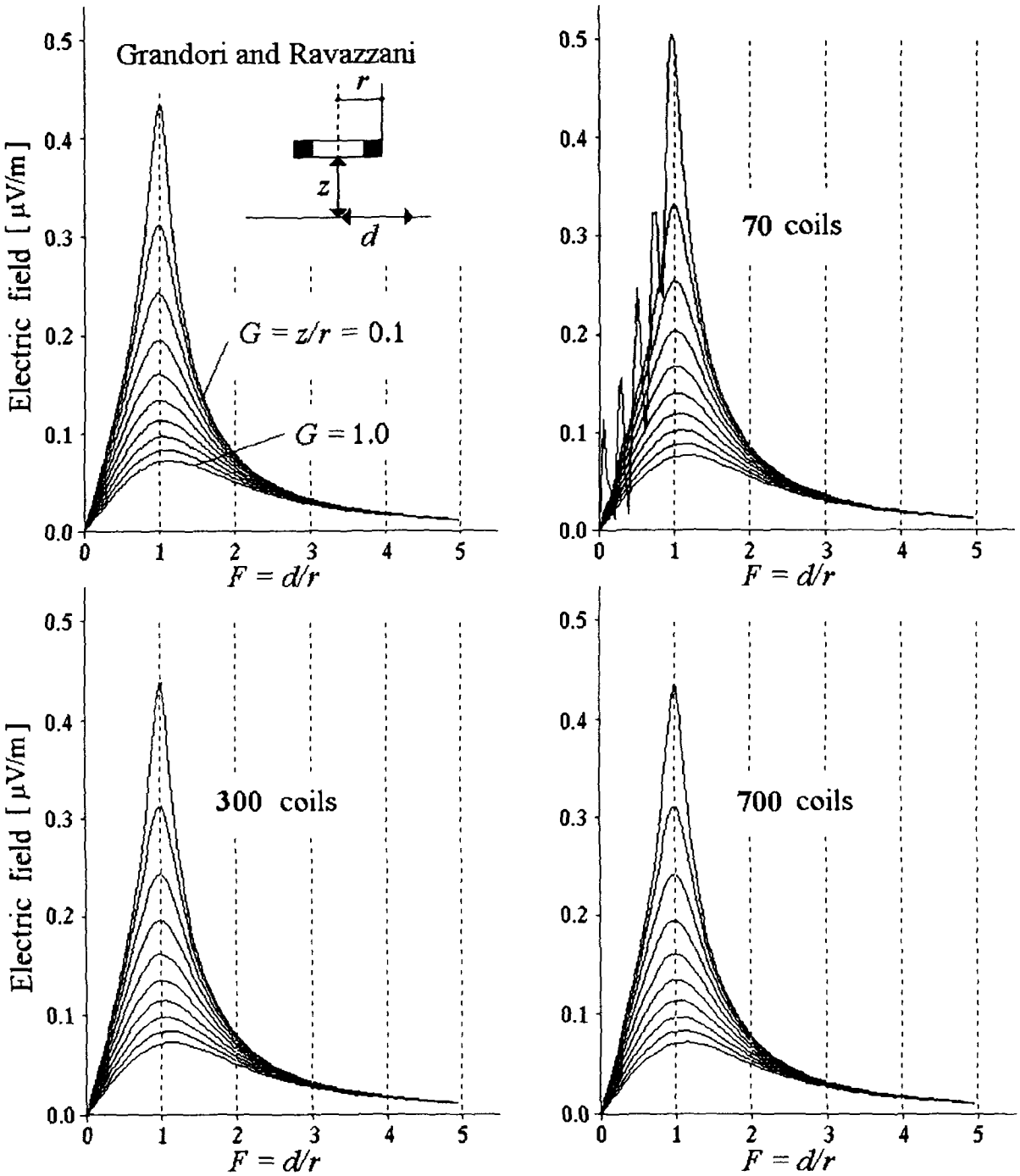

FIGURE 1. Magnitude of the induced electric field computed with the *reciprocity* model along a line parallel to the coil plane at different depths. The coil area is divided into n = 70, 300, or 700 subareas. At the top left is an exact closed-form solution to E (adapted from Grandori and Ravazzani (10)). The field point is at distance d from the coil axis and at depth z below the coil plane; both are normalized to the coil radius: $F = d/r$ and $G = z/r$, respectively. di/dt = 1 A/s.

with magnetic moment $\mathbf{m}$ at $\mathbf{r}_m$ outside the medium and an infinitesimal current dipole $\mathbf{Q}$ at $\mathbf{r}_Q$ inside the volume conductor V. The current density $\mathbf{J}_m^p$ in the coil causes the electric field $\mathbf{E}_m$, and the current dipole $\mathbf{Q}$ causes the electric field $\mathbf{E}_Q$. Applying the reciprocity theorem and Faraday's law, one can obtain

$$\mathbf{Q} \cdot \mathbf{E}_m(\mathbf{r}_Q) = ji\omega\Phi(S), \qquad (1)$$

where i is the current in the coil loop, and $\Phi(S)$ is the magnetic flux linking the circuit C, *i.e.*, the flux $\Phi(S)$ through the coil surface S produced by the current dipole $\mathbf{Q}$. The imaginary unit j represents the phase difference between the coil current and the induced electric field.

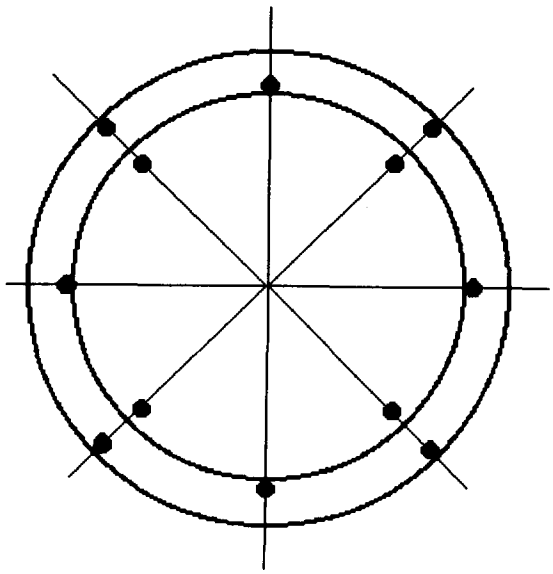

FIGURE 2. Pictorial representation of the location of the 12 points r_k. The values of r_k and da_k for the optimized 12-point integration are given in Table 1.

The coil surface S is divided into subsurfaces dS sufficiently small so that $\mathbf{B}$ can be considered constant on each of them (discretization of the flux integral is discussed further in the next section). Recalling that $\mathbf{n}$ is the unitary vector normal to dS and $\mathbf{m} = iS\mathbf{n}$, one can obtain

$$\mathbf{Q} \cdot \mathbf{E}_m(\mathbf{r}_Q) = j\omega \mathbf{m} \cdot \mathbf{B}_Q(\mathbf{r}_m). \quad (2)$$

TABLE 1. Parameters for the 12-point integration formula.

r_k			
θ_k	r_k	da_k	k
$\left(k-\frac{1}{2}\right)\frac{\pi}{2}$	$0.45667c$	$0.12321\pi c^2$	$k = 1, \ldots, 4$
$k\frac{\pi}{2}$	$0.86603c$	$0.074074\pi c^2$	$k = 5, \ldots, 8$
$\left(k-\frac{1}{2}\right)\frac{\pi}{2}$	$0.91100c$	$0.052715\pi c^2$	$k = 9, \ldots, 12$

From Ref. 17.

By vectorial algebra it is easy to show that $\mathbf{E}_m(\mathbf{r}_Q)$ can be expressed by

$$\mathbf{E}_m(\mathbf{r}_Q) = j\omega \frac{\mathbf{m} \cdot \mathbf{B}_Q(\mathbf{r}_m)}{\mathbf{Q} \cdot \mathbf{Q}} \mathbf{Q}. \quad (3)$$

More accurate details on the model and the complete solutions for unbounded, semi-infinite, spherical, and cylinder-like media can be found in the literature (11,13, 18,19).

Discretization of the Flux Integral

In magnetic stimulation, coils usually have an outer radius greater than 5 cm, and therefore $\mathbf{B}$ cannot be assumed to be constant on their whole surface S. Thus, in previous discussions, $\Phi(S)$ should be computed from its

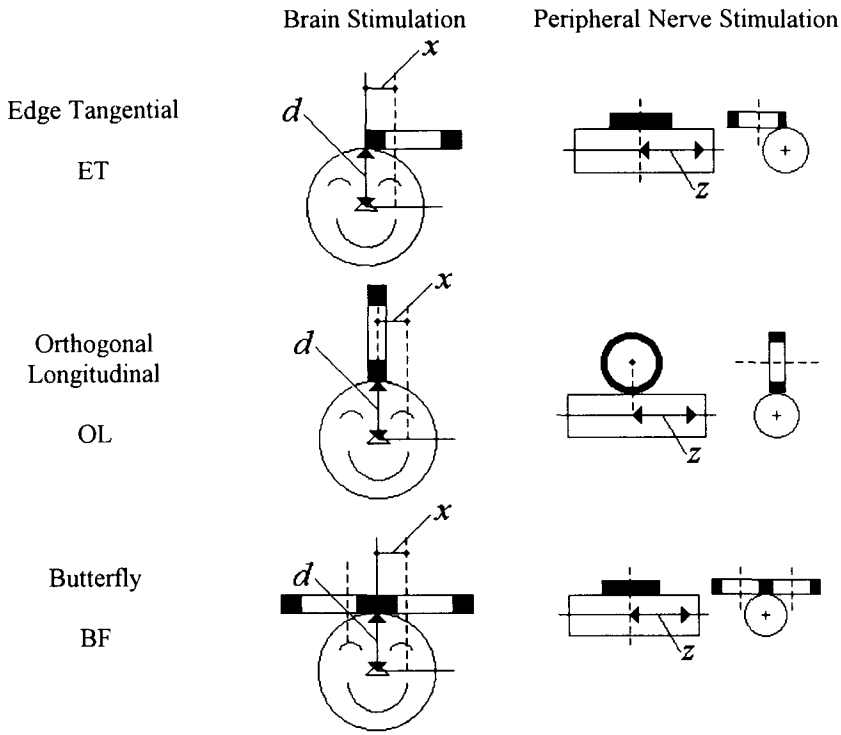

FIGURE 3. Typical coil arrangements for cortical and peripheral magnetic stimulation. In peripheral nerve stimulation the nerve is directed along the *z* axis.

classical complete formulation, in such a way that the advantages of that approach are at least partially lost. Actually, the flux caused by a current source should be computed by numerical integration of **B** or the vector potential, but this can be time consuming. Usually the coil area is discretized into n points and the flux is computed from

$$\Phi^* = \sum_{k=1}^{n} \mathbf{B}(\mathbf{r}_k) \cdot \mathbf{n}(\mathbf{r}_k) da_k, \qquad (4)$$

where $\Phi^* \rightarrow \Phi$, when $n \rightarrow \infty$ in every subregion $\mathbf{n}(\mathbf{r}_k)$. The weighting factor of point $\mathbf{r}_k$ is da_k. Practically, the coil area is divided into n small current loops with a magnetic moment $\mathbf{m}_n$, each carrying the same current $i(t)$ as the coil. The induced electric field $\mathbf{E}_m(\mathbf{r}_Q)$ is then evaluated by linear superposition. The sum is truncated for a sufficiently great value of n, which can be estimated by testing Eq. 4 with different coil configurations. In Fig. 1 the induced **E** is computed along a line parallel to the coil plane in unbounded space as a function of n and compared with an exact closed-form solution (10). A small n results in an apparent error (top right of Fig. 1), which decreases with increasing n. When $n = 300$, the error is insignificant. In addition, the greater the distance is from the coil plane, the lower becomes the error. The relative error in **E** in spherical volume as a function of n can be estimated, taking the **E** computed with $n = 2000$ as the reference value. In simulations, a coil with a radius from 4 to 10 cm was placed tangential to the sphere, with its axis pointing to the sphere center. The electric field was computed along a line parallel to the coil plane, starting from the coil axis. The line was 1.2 cm from the coil plane, corresponding approximately to the distance between the cerebral tissue and the scalp (21). For any coil radius the error was smaller than 1% when n exceeded 300 and vanished with greater values. Interestingly, the error did not decrease monotonically with n, probably because of unoptimally chosen $\mathbf{r}_k$. For other coil orientations the convergence was found to be more rapid.

An optimization procedure that allows the magnetic field to be quickly integrated over the coil area has been proposed by Roth and Sato (17). They assumed that a circular coil of radius c lies in the polar $r\theta$ plane. The flux through the coil is approximated by the weighted sum in Eq. 4. In this approach, the coil area is divided into 12 optimally chosen sections da_k, and **B** is computed in the 12 points $\mathbf{r}_k$, as shown in Fig. 2. The 12-point integration gives accurate values of **E** (relative error <1%) when the coil is farther than 2 cm from the computation points, whereas at shorter distances the error increases by up to

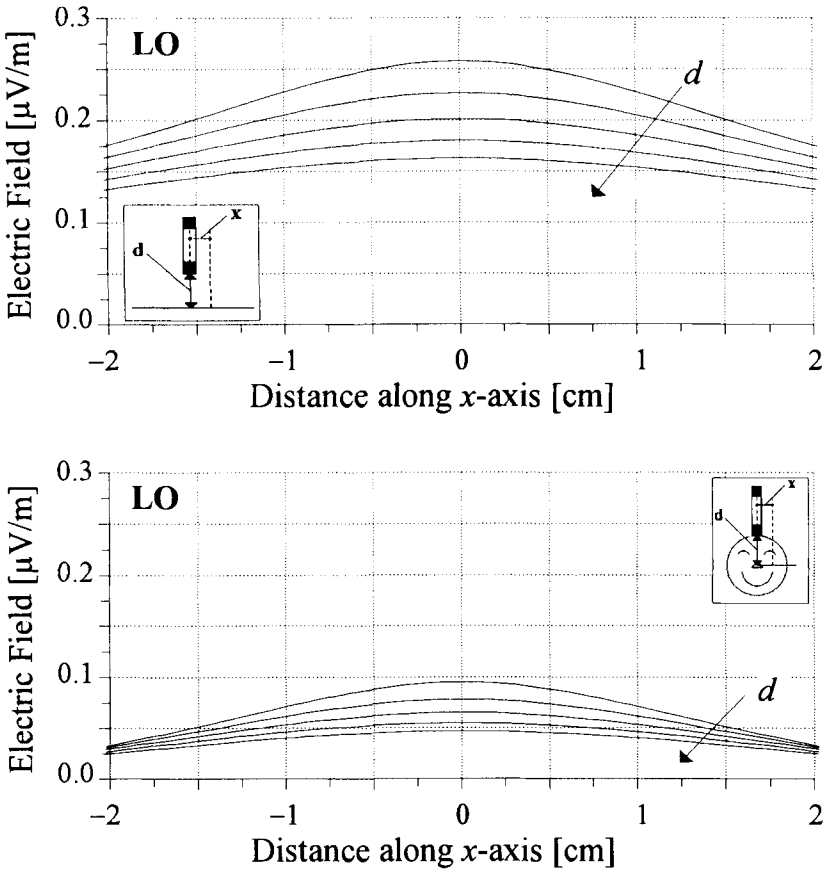

FIGURE 4. Comparison between the magnitude of E inside unbounded (top) and spherical (bottom) medium. The OL orientation is considered. The field is computed along lines parallel to the *x* axis at depths *d* = 1.5, 1.8, 2.1, 2.4, and 2.7 cm (the arrows point toward deeper lines). The lines are perpendicular to the coil plane, and the edge of the coil is at *x* = 0 cm. The coil radius is 5 cm, and the rate of change of the current is 1 A/s.

20–30%. If the distance is shorter than 1 cm (down to 0.5 cm), computation of **E** with an error of 3% is still obtained when the coil surface is normal to the surface of the medium (OL, orthogonal-longitudinal arrangement; see also below).

COIL ARRANGEMENTS AND ORIENTATIONS

In the comparison of the effects of the medium boundaries on the induced electric field, different coil arrangements and orientations that are common in the clinical use of magnetic stimulation have to be taken into account.

Adapting the terminology of Evans (9), we call the different arrangements of the single coil in peripheral nerve stimulation the edge-tangential (ET) arrangement and the orthogonal-longitudinal (OL) arrangement. The ET arrangement refers to the case with the coil plane parallel to the skin surface and one edge along the nerve; the OL arrangement refers to the case with the coil plane perpendicular to the tissue surface and one edge along the nerve. These definitions are also valid in motor cortex magnetic stimulation.

When the double coil (or butterfly (BF), as in the rest of the paper) is used, its orientation is simply defined by the relative position of the overlapping edges of the coils (that is, of the stimulator handle) with respect to either the nerve or the cortical target area. Figure 3 illustrates these typical coil arrangements for both cortical and peripheral magnetic stimulation.

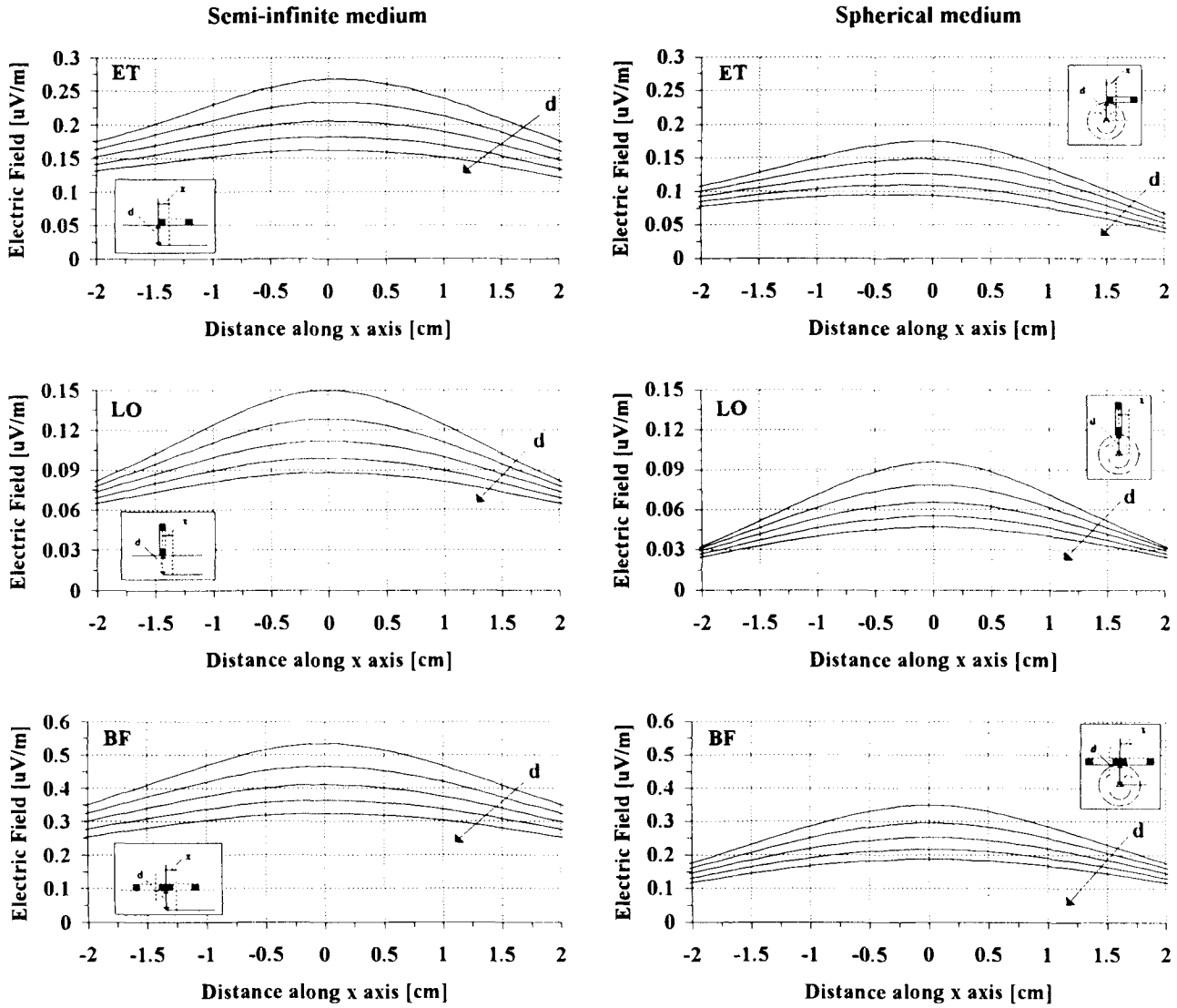

FIGURE 5. Comparison between the magnitude of E induced by different coil orientations (ET, OL, BF). The brain is modeled as a semi-infinite medium (left) and as an 8-cm-radius sphere (right). E is computed along *x*-axial lines parallel to the coil plane for the ET and BF arrangements and perpendicular for the OL arrangement. Other details are as in Fig. 4.

TABLE 2. Focusing length.

	ET		OL		BF	
Depth (cm)	Sphere	Semi-inf.	Sphere	Semi-inf.	Sphere	Semi-inf.
1.5	2.9	2.3	2.4	2.2	2.4	2.4
1.8	3.2	2.5	2.4	2.4	2.6	2.4
2.1	3.3	2.6	2.6	2.5	2.6	2.4
2.4	3.3	2.7	2.6	2.5	2.7	2.6
2.7	3.3	2.8	2.6	2.6	2.7	2.6

Data are in centimeters.

Here, all computer simulations consider exclusively the spatial rather than temporal characteristics of the induced electric field. Hence, the rate of change of the current in the stimulating coil is assumed to be 1 A/s for brain stimulation and 100 A/μs for peripheral nerve stimulation. In all cases circular 5-cm-radius coils are considered; the magnetic flux through the coil area is integrated with discretizing the coil into 300 subareas; in peripheral nerve stimulation, the optimized 12-point routine is used.

BRAIN STIMULATION

It is well known that surface charges, which contribute to the induced electric field, are less important when the coil plane is tangential rather than perpendicular to the volume-conductor boundary near the coil. In other terms, one can expect that the greatest differences between simplified and more realistic geometries occur when the coil plane is not tangentially oriented to the surface. Figure 4 shows the magnitude of the induced electric field **E** along lines perpendicular to the plane of the OL coil, for the unbounded and spherical media. The electric fields behave similarly, but because of the charges on the sphere surface, the maximum of **E** in the sphere is only about 30–

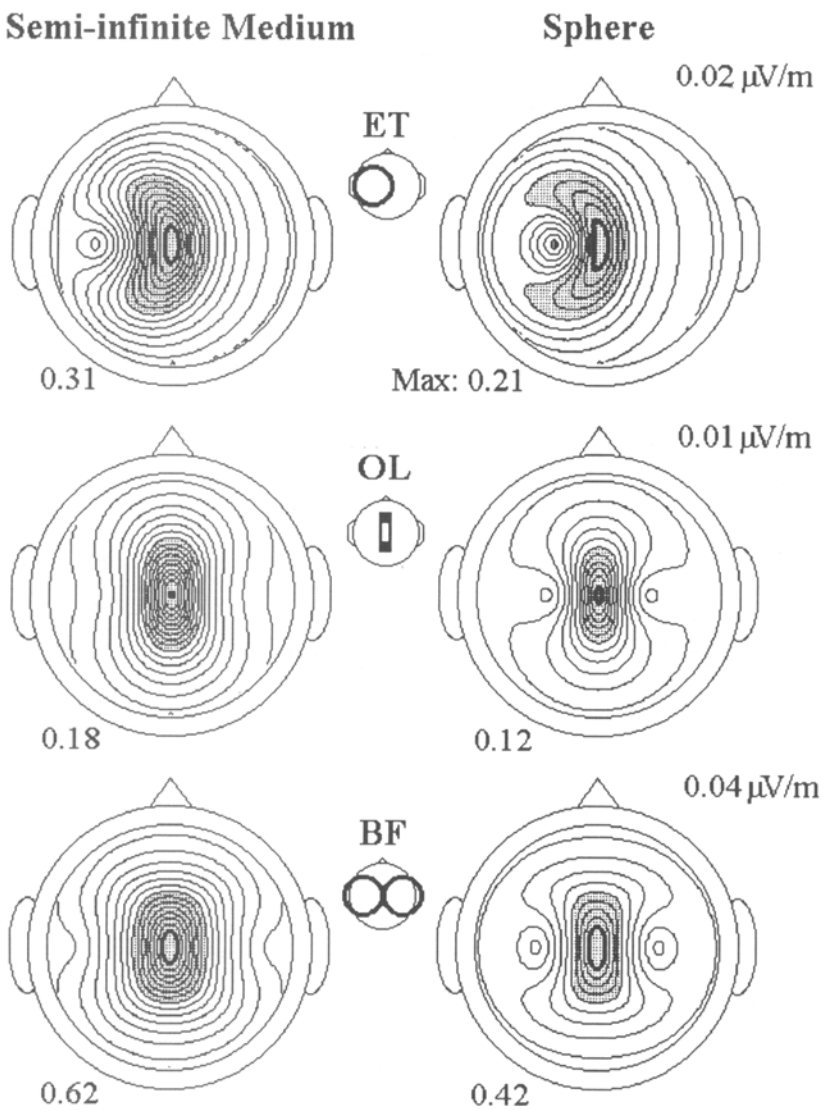

FIGURE 6. Isolevel maps of the magnitude of E on spherical surfaces for the semi-infinite (left) and spherical (right) medium. In the sphere, the spherical surface is concentric with the sphere. The radii of the coil are 5 cm and the rate of change of the current is 1 A/s. Maximum of the field is given at the bottom of each map. Dashed areas indicate the regions where the magnitude of E exceeds the half-maximum value. The depth of the spherical surface from the scalp is 1.2 cm. Contour step is given at top right of each pair of maps.

40% of the corresponding unbounded value, depending on the target depth.

In Fig. 5 the magnitude of **E** in the semi-infinite and spherical media is computed for different coil arrangements. As previously, the maximum of **E** is again markedly less in the sphere than in the semi-infinite medium; in the sphere **E** is only about 50–65% of the corresponding semi-infinite value, depending on the target depth and on the coil arrangement.

We define the focusing length as the length of the segment of an x-axial line over which **E** is over its half-maximum value. Focusing length gives a quantitative measure of the capability of focusing the field, a small value indicating a good focality.

Table 2 shows the focusing length in the sphere and in the semi-infinite medium as a function of depth for the three arrangements (ET, OL, BF). As one may expect, whichever geometry is used for the model, the focusing length decreases with decreasing depth; in other words, focusing is better near the coil. The semi-infinite model underestimates the focusing length. The focusing capability is best for the OL arrangement and worst for the ET arrangement. Focality of the BF arrangement is slightly worse than that of the OL arrangement.

The spatial behavior of the induced **E** in the motor cortex can be more effectively analyzed when **E** is computed and visualized on spherical surfaces instead of on planes or along straight lines. Figure 6 shows the magnitude of **E** on a spherical surface inside a semi-infinite and a spherical medium for different coil arrangements. The fields are shown as isolevel contours projected on the plane defined by the nasion and the ear canals. The dashed areas represent the regions of the cortex where the magnitude of **E** exceeds its half-maximum value. Apart from the lower magnitudes in the sphere (about 67% of the unbounded case), the isolevel maps have considerably dif-

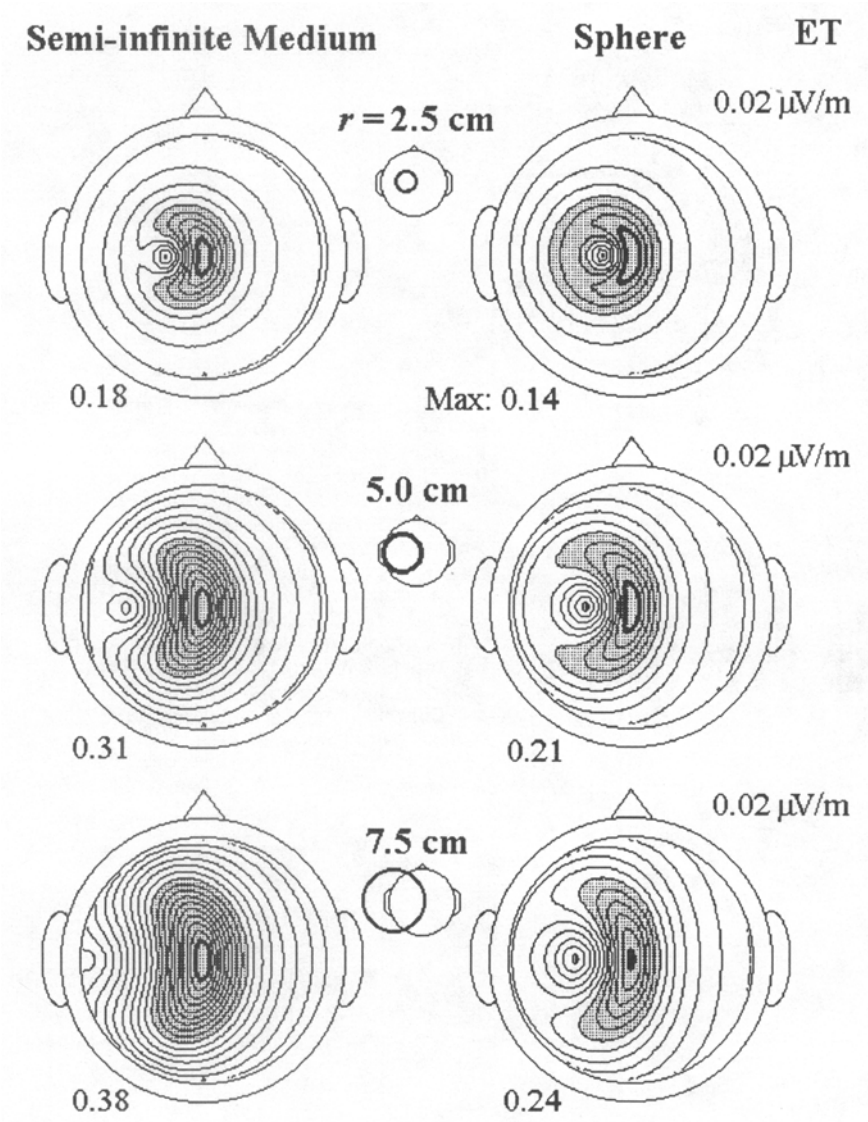

FIGURE 7. Isolevel maps of the magnitude of E on spherical surfaces for ET coils of different radii, for the semi-infinite (left) and spherical (right) medium. The coil radii from top to bottom are r = 2.5, 5, and 7.5 cm. Isolevel spacing is 0.02 μV/m. Other details are as in Fig. 6.

ferent pattern. For all arrangements, the shape and the dimension of the dashed area in the sphere differ strongly from the corresponding area in the semi-infinite medium.

In Fig. 7 are shown the effects of changing the coil radius. The isolevel maps show a decrease in magnitude with decreasing coil radius, but also a different pattern. In particular, the largest coil (radius of 7.5 cm) induces a markedly more focused **E** in the sphere than in the semi-infinite medium.

PERIPHERAL NERVE STIMULATION

The aim of neural stimulation is to depolarize the cell membrane in such a way that the membrane potential exceeds a threshold value and the neuron generates a propagating depolarization front or an action potential. Among others, Roth and Basser (14) have predicted that a z-axial axon is depolarized where the z-axial gradient E_z' of the z-component of **E** is most negative. In other words, the magnitude, sign, and time course of the spatial derivative of the component of **E** along the axon should determine whether and where the excitation occurs. Actually, this view is only in partial agreement with experiments; recently, strong evidence of excitation of a peripheral nerve with such coil locations and orientations that do not produce E_z' within the nerve has been demonstrated by Ruohonen and colleagues (20). By comparing the theory with experimental data, they concluded that the component of **E** transverse to the nerve also produces excitation. However, the discussion will be limited here to the consideration of only such situations in which the mechanism of excitation is thought to depend solely on E_z'.

Figures 8, 9, and 10 show E_z' in unbounded, semi-infinite, and cylindrical media for the ET, OL, and BF arrangements, respectively. The cylindrical medium is a 50-cm-long and 8-cm-thick prolate spheroid. The magnitude of **E** has been computed both on a longitudinal plane as isolevel lines and along straight lines that are parallel to the axon at different depths from the coil plane. For the ET and BF arrangements, in all geometries the pattern and the maximum value of the fields are similar. Only in the case of the OL arrangement (Fig. 10) is remarkable variation in E_z' with the volume-conductor shape observed; both the pattern of E_z' on longitudinal planes and its absolute values along the axon vary with the geometry.

In peripheral nerve stimulation it is useful to refer to the site where maximum membrane depolarization occurs as the virtual cathode and the site of maximum hyperpolarization as the virtual anode. The virtual cathode corre-

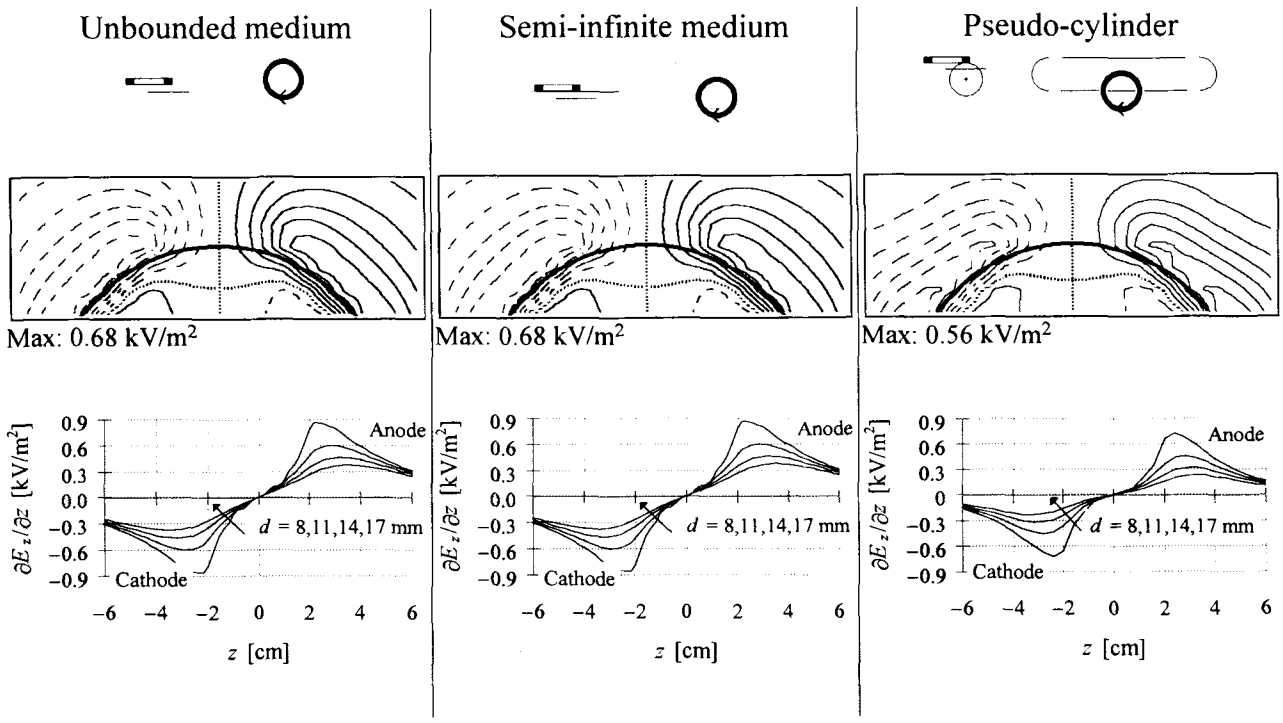

FIGURE 8. E_z', ***i.e.***, **the gradient of E along the axon, for the ET arrangement in the unbounded, semi-infinite, and cylindrical medium. The top panels show isolevel maps of E_z'; the bottom panels give E_z' along a z-axial axon at depths d = 0.8, 1.1, 1.4, and 1.7 cm. The maps correspond to 12-cm-wide rectangular planes 10 mm below the 5-cm-radius coil that touches the conductor surface. The contour step is 0.1 kV/m². The zero contour line is dotted and the negative contours are dashed. The thickest line is the projection of the coil on the plane. The inserts show the arrangements as seen from the direction of the positive z-axis and from the top. The rate of change of the current is 100 A/μs.**

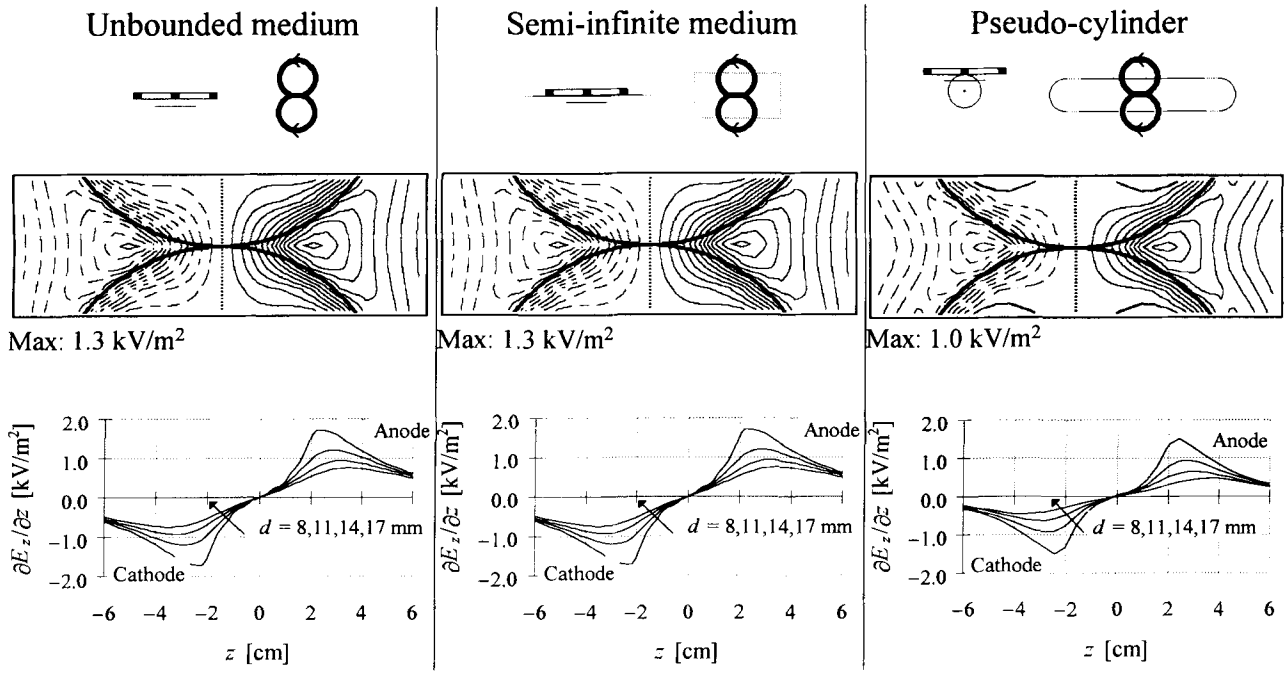

FIGURE 9. E'_z **for the BF arrangement in the unbounded, semi-infinite, and cylindrical medium. Details are as in Fig. 8.**

sponds to the negative maximum of E'_z, the virtual anode to the positive maximum of E'_z. The distance between the virtual anode and cathode along the axon can be easily estimated experimentally (19). Theoretical values of the anode-cathode separation have been computed for the ET, OL, and BF arrangements and are given in Table 3. The anode-cathode separation depends on the selected geometry only in the case of the OL arrangement; in the cylindrical approximation, the anode-cathode separation is 1–2 cm shorter than in other conductors. For the ET and BF

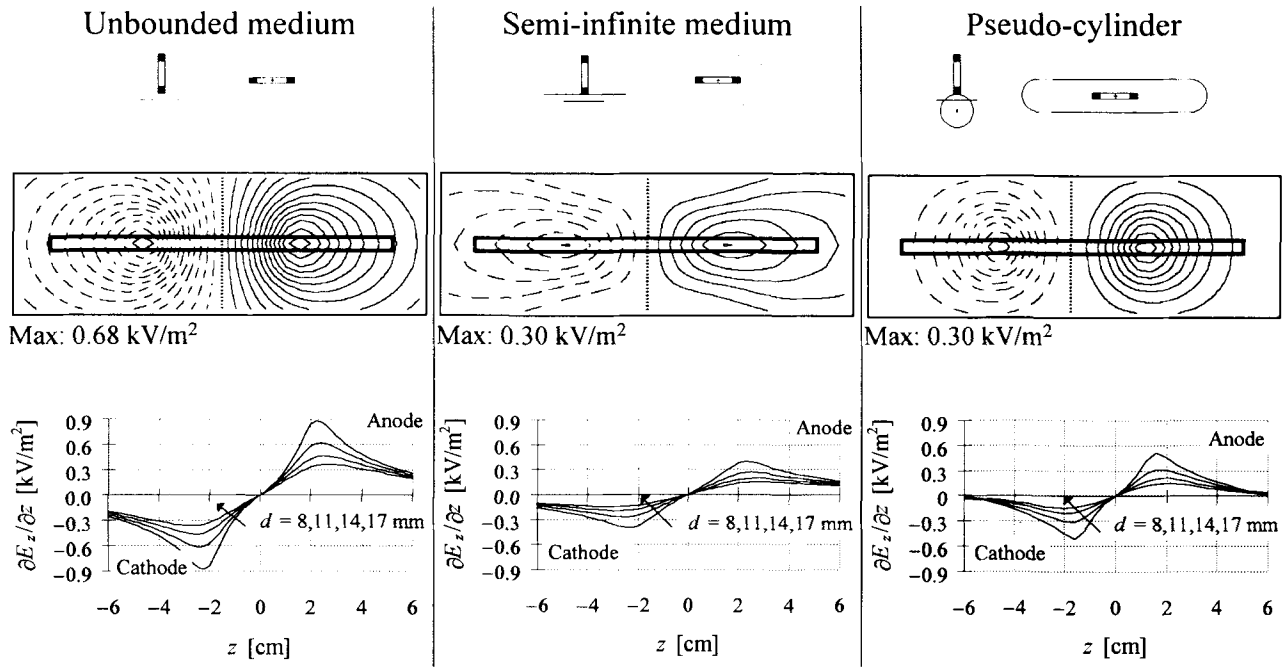

FIGURE 10. E'_z **for the OL arrangement in the unbounded, semi-infinite, and cylindrical medium. The contour step is 0.05 kV/m². Other details are as in Fig. 8.**

arrangements, practically no differences were found, suggesting that the volume conductor shape has only a small influence on the site of excitation, if any.

DISCUSSION

So far, many analytical models have been developed and used to compute the electric field induced by magnetic stimulation of the nervous system. Because of their intrinsic simplicity, in most applications unbounded and semi-infinite models have been used to obtain approximate results (2,5,7,10,12,23). However, these models have been used somewhat blindly, without any *a posteriori* validation of their reliability. A comparison of approximated and more realistically shaped models becomes crucial to better interpretation and understanding of the outcome of experimental magnetic stimulation; in addition, it is useful to know the cases in which the influence of conductor boundaries is small enough to allow the use of more simplified models.

For what concerns motor cortex magnetic stimulation, the magnitude of the electric field may be greatly overestimated by the use of the unbounded or semi-infinite medium instead of the sphere. This can result in erroneous interpretations when the models are used to study the mechanism and site of activation in brain stimulation or to compare the relative merits of different stimulation procedures.

In this study the focusing length was introduced to evaluate the focality of different coils and their orientations. The capability of focusing the stimuli appears to be worse in the sphere than in the more simplified models; the focusing length in the sphere is greater by up to 10% for the OL and BF arrangements and by about 20% for the ET arrangement. For the ET arrangement the result is due to asymmetry in **E** along the target line in the spherical medium (top right panel in Fig. 5). Furthermore, the analysis of the topographic distribution of the induced electric field leads to a similar conclusion. Importantly, the pattern of **E** is extremely different for the ET arrangement in the spherical medium: **E** is less focused and a larger area is involved in stimulation. This explains the well-known result from clinical practice that the ET configuration is the easiest way to obtain motor cortex magnetic stimulation without any *a priori* knowledge of the location of the target area.

TABLE 3. Anode-cathode separation.

Depth [cm]	Unbounded	Semi-infinite	Cylinder[a]
	ET arrangement		
0.8	4.8	4.8	4.8
1.1	5.8	5.8	5.6
1.4	6.4	6.4	6.0
1.7	7.0	7.0	6.8
	BF arrangement		
0.8	4.8	4.8	4.8
1.1	5.8	5.8	5.6
1.4	6.4	6.4	6.0
1.7	7.0	7.0	7.2
	OL arrangement		
0.8	4.4	4.8	3.2
1.1	4.8	5.2	3.2
1.4	5.2	5.4	4.0
1.7	5.4	6.0	4.0

[a]100-cm-long and 8-cm-thick prolate spheroid.
Values are in centimeters.

The influence of the coil radius is higher when a more realistic geometry is considered. A small coil is able to excite smaller cortical structures than a larger coil, but with marked changes in the shape of the stimulated areas when the spherical conductor shape is assumed; in Fig. 7 a 7.5-cm-radius coil induces an **E** about twice as high as that of a 2.5-cm-radius coil, together with great changes in the pattern. In the semi-infinite medium only the magnitude, and not the pattern, changes as a function of the coil radius.

For what concerns peripheral nerve stimulation, the conductor geometry has no significant influence for the ET and BF arrangements. Only the OL configuration is sensitive to geometrical simplification of the conductor geometry, causing significant changes in the field pattern, magnitude, and anode-cathode separation. In clinical practice, however, with the OL configuration it is difficult or even impossible to attain nervous excitation, because of the limited output power of the currently available stimulators.

To summarize, for magnetic stimulation of the cortical structures the use of highly simplified volume-conductor models is not advisable. Nothing is gained in computation time, and all models that we presented for cortical stimulation typically take just seconds in a personal computer. For peripheral nerve stimulation the use of the unbounded or semi-infinite medium is advantageous for coil configurations typically used in clinical practice. Actually one has to take into account that the estimation of **E** by means of the cylindrical model is costly in terms of computation time.

The same considerations of computation time hold also for what concerns the discetization of the flux integral computed on the surface S of the coil. When unbounded, semi-infinite, and spherical media are considered, one can rely upon the conventional unoptimized procedure, since in these cases the computation of **B** over 300 points takes just seconds for any coil arrangement. In contrast, when the cylindrical medium is considered, the computation over 300 coils may be time consuming, and hence the use of the optimized 12-point integration procedure would be advisable, at least when the coil plane is not closer than 15 mm to the field point and the coil radius is not greater than about 3 cm.

ACKNOWLEDGMENT

This work has been partially coordinated within the framework of the program "Functional substitutions, artificial organs and transplants" of the Italian Istituto Superiore di Sanità (project STIMAG on magnetic stimulation of the nervous system).

REFERENCES

1. Barker, A. T., R. Jalinous, and I. L. Freeston. Non-invasive magnetic stimulation of human motor cortex. *Lancet* 1:1106–1107, 1985.
2. Cohen, D., and B. N. Cuffin. Developing a more focal magnetic stimulator. Part I: Some basic principles. *J. Clin. Neurophysiol.* 8:102–111, 1991.
3. Cuffin, B. N., and D. Cohen. Magnetic fields of a dipole in special volume conductor shapes. *IEEE Trans. Biomed. Eng.* 24:372–382, 1977.
4. De Leo, R., G. Cerri, D. Balducci, F. Moglie, O. Scarpino, and M. Guidi. Computer modeling of brain cortex excitation by magnetic field pulses. *J. Med. Eng. Tech.* 16:149–156, 1992.
5. Durand, D., A. S. Ferguson, and T. Dalbasti. Effect of surface boundary on neuronal magnetic stimulation. *IEEE Trans. Biomed. Eng.* 39:58–64, 1992.
6. Eaton, H. Electric field induced in a spherical volume conductor from arbitrary coils: Applications to magnetic stimulation and MEG. *Med. Biol. Eng. Comput.* 30:433–440, 1992.
7. Esselle, K. P., and M. A. Stuchly. Neural stimulation with magnetic fields: Analysis of induced electric fields. *IEEE Trans. Biomed. Eng.* 39:693–700, 1992.
8. Esselle, K. P., and M. A. Stuchly. Quasi-static electric field in a cylindrical volume conductor induced by external coils. *IEEE Trans. Biomed. Eng.* 41:151–158, 1994.
9. Evans, B. A. Magnetic stimulation of the peripheral nervous system. *J. Clin. Neurophysiol.* 8:77–84, 1991.
10. Grandori, F., and P. Ravazzani. Magnetic stimulation of the motor cortex—theoretical considerations. *IEEE Trans. Biomed. Eng.* 38:180–191, 1991.
11. Heller, L., and D. B. van Hulsteyn. Brain stimulation using electromagnetic sources: Theoretical aspects. *Biophys. J.* 63:129–138, 1992.
12. Nagarajan, S. S., D. M. Durand, and E. N. Warman. Effects of induced electric fields on finite neuronal structures: A simulation study. *IEEE Trans. Biomed. Eng.* 40:1175–1188, 1993.
13. Ravazzani, P., J. Ruohonen, and F. Grandori. Magnetic stimulation of peripheral nerves: Computation of the induced electric fields in a cylinder-like structure. *Adv. Eng. Software* 22:29–35, 1995.
14. Roth, B. J., and P. J. Basser. A model of the stimulation of a nerve fiber by electromagnetic induction. *IEEE Trans. Biomed. Eng.* 37:588–597, 1990.
15. Roth, B. J., L. G. Cohen, M. Hallett, W. Friauf, and P. J. Basser. A theoretical calculation of the electric field induced by magnetic stimulation of a peripheral nerve. *Muscle Nerve* 13:734–741, 1990.
16. Roth, B. J., J. M. Saypol, M. Hallett, and L. G. Cohen. A theoretical calculation of the electric field induced in the cortex during magnetic stimulation. *Electroencephalogr. Clin. Neurophysiol.* 81:47–56, 1991.
17. Roth, B. J., and S. Sato. Accurate and effective formulas for averaging the magnetic field over a circular coil. In: *Biomagnetism: Clinical Aspects*, edited by M. Hoke, S. N. Ernè, Y. C. Okada, and G. L. Romani. Amsterdam: Excerpta Medica, Elsevier, 1992, pp. 797–800.
18. Ruohonen, J., P. Ravazzani, and F. Grandori. An analytical model to predict the electric field and excitation zones due to magnetic stimulation of peripheral nerves. *IEEE Trans. Biomed. Eng.* 42:158–161, 1995.
19. Ruohonen, J., P. Ravazzani, J. Nilsson, M. Panizza, F. Grandori, and G. Tognola. A volume-conduction analysis of magnetic stimulation of peripheral nerves. *IEEE Trans. Biomed. Eng.* 43:669–678, 1996.
20. Ruohonen, J., M. Panizza, J. Nilsson, P. Ravazzani, F. Grandori, and G. Tognola. Transverse-field activation mechanism in magnetic stimulation of peripheral nerves. *Electroencephalogr. Clin. Neurophysiol.* 101:167–174, 1996.
21. Rush, S., and D. A. Driscoll. Current distribution in the brain from surface electrodes. *Anesth. Analg.* 47:717–723, 1968.
22. Sarvas, J. Basic mathematical and electromagnetic concepts of the biomagnetic inverse problem. *Phys. Med. Biol.* 32: 11–22, 1987.
23. Tofts, P. S. The distribution of induced currents in magnetic stimulation of the nervous system. *Phys. Med. Biol.* 35: 1119–1128, 1990.
24. Ueno, S., T. Tashiro, S. Kamise, and K. Harada. Localised hyperthermia by means of a paired-coil configuration: Calculation of current distributions in cubical model. *IEEE Trans. Magn.* 23:2437–2439, 1987.
25. Ueno, S., T. Tashiro, and K. Harada. Localised stimulation of neural tissues in the brain by means of a paired configuration of time-varying magnetic fields. *J. Appl. Physiol.* 64:5862–5864, 1988.
26. Yonokuchi, K., D. Cohen, and B. N. Cuffin. Borrowing concepts from biomagnetism in developing a focal magnetic stimulator. Proceedings of the 7th International Conference on Biomagnetics, New York, August 14–18, 1989, pp. 161–162 1989